402 423

TRANSLATION

EXPERIMENTAL STUDY OF THE TURBULENT BOUNDARY
LAYER IN GAS MOTION IN AXISMMETRICAL
DIFFUSERS WITH COOLED WALLS

BY

P. N. Romanenko and A. I. Leont'yev

FOREIGN TECHNOLOGY
DIVISION

AIR FORCE SYSTEMS COMMAND

WRIGHT-PATTERSON AIR FORCE BASE

OHIO
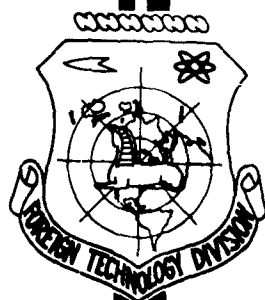
402 423
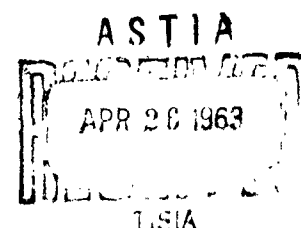
UNEDITED ROUGH DRAFT TRANSLATION

EXPERIMENTAL STUDY OF THE TURBULENT BOUNDARY LAYER
IN GAS MOTION IN AXISMMETRICAL DIFFUSERS WITH
COOLED WALLS

By: P. N. Romanenko and A. I. Leont'yev

English Pages: 31

SOURCE: Russian Book, Moskovskogo Instituta
Inzhenerov, Zhelesnoderoshnyy Transport,
Nr. 139, 1961, pp. 134-158

(Ref. In) S/196-62-0-14

EXPERIMENTAL STUDY OF THE TURBULENT BOUNDARY LAYER

IN GAS MOTION IN AXISYMMETRICAL DIFFUSERS

WITH COOLED WALLS

P. N. Romanenko and A. I. Leont'ev

1. Statement of Problem

The study of turbulent boundary-layer characteristics under
conditions of significant longitudinal pressure and heat-transfer
gradients is of great practical value for the development of engi-
neering methods to calculate friction and heat transfer in modern
industrial installations and to elucidate turbulent mixing under
these conditions.

The published works on the investigation of the turbulent
boundary layer in the presence of significant pressure gradients
[1, 2, 5, 6, 12] are mainly concerned with the dynamic boundary layer.
The well-known semi-empirical methods of calculating an isothermal
turbulent boundary layer in the region of significant pressure gradients
permit sufficiently reliable calculation of the dynamic characteristics
of the turbulent boundary layer and enable us to determine the location
of separation points of the turbulent boundary layer. However, the
expansion of these methods to the calculation of a turbulent boundary
layer under conditions of intense turbulence presently remains an

open question. Methods of computing the thermal boundary layer which are sufficiently expanded in engineering practice [13], based on the use of the analogy between the processes of heat and momentum transfer and also on the self-similarity of the laws of friction and heat transfer in the region of significant positive gradients of pressure, are still inapplicable. Studies in which attempts were made to calculate theoretically, the influence of pressure gradients on the dynamic and thermal characteristics of boundary layers are well known [14]. However, the large number of poorly founded assumptions and inexcusably cumbersome formulas significantly reduce the practical value of the methods of computation proposed in these works.

Since in the near future we cannot count on serious progress in the application of statistical theories to the study of anisotropic turbulence, experimentation must be acknowledged as the most effective method of study.

This work presents the results of studies of the turbulent boundary layer in heated air flow in diffusers of circular cross-section with cone angles of 8°4' and 12°. The axisymmetrical diffuser makes it possible to eliminate the effect on calculations of the local resistance coefficient and of other flow characteristics of a three-dimensional gas flow which, as was demonstrated by F. Clauser [3], takes place in flat diffusers. The use of experimental data obtained for a flat diffuser hampers the calculation of the resistance coefficient with respect to the integral relation of momenta. In addition, the study of the axisymmetrical flow gradient is of great practical interest.

2. Experimental Installation

A general schematic of the experimental installation is shown in

Fig. 1. It consists of an open wind tunnel of periodic action with detachable nozzles and a test section. In addition, the apparatus includes: a 2R-4/220 air compressor which produces 180 m³/hr (NTP) (final air pressure of 220 atm (abs), an 80-tank receiver, a 300 Kw electric heater, an arrangement for the enclosure and feeding of ejected air to the chamber, a system for water cooling the test section, and measuring devices.
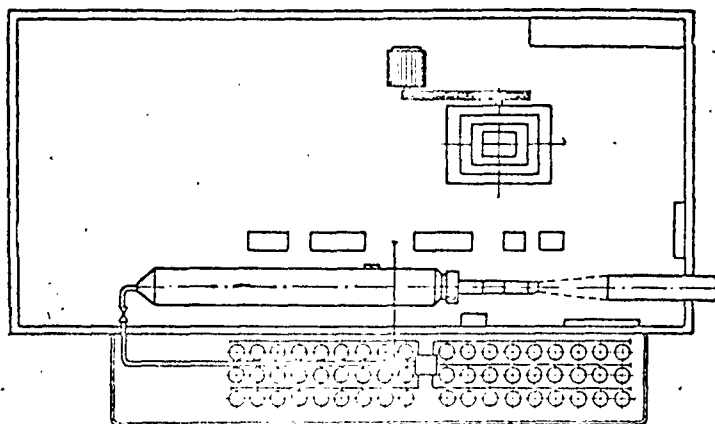
Fig. 1. Schematic of experimental installation.

Figure 2 shows a longitudinal cross section of the experimental device, an axisymmetrical diffuser with a 4°2' cone half-angle. The profiles in which static and total pressures as well as temperatures of the flow were measured are marked. A structural cross section of the sleeve through which the Pitot microtube and thermocouples are introduced into the channel is shown.

The diffuser is composed of five insulated sections with double walls which form a space through which cooling water is passed. The water flow rate is determined by the gravimetric method. The internal wall is made of 2 mm-thick copper and the exterior wall of 2.5 mm steel.
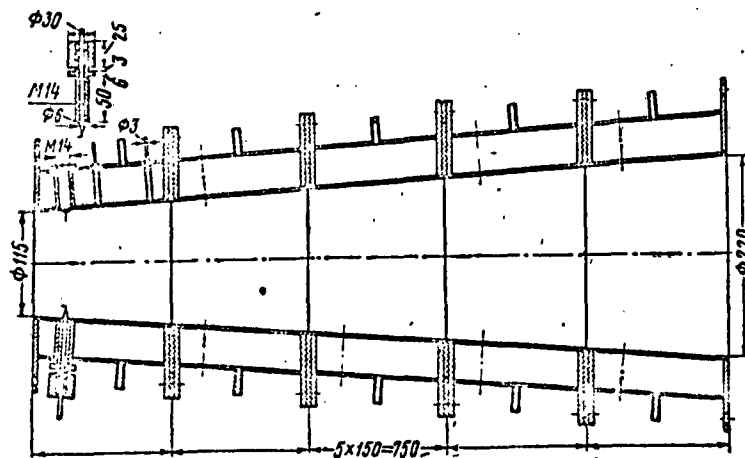
Fig. 2. Longitudinal cross section of the
test section.

The compressed air is forced from the compressor into the receiver
whose tanks are joined by prefabricated ramps into six groups. Each
group of tanks is connected to a high-pressure delivery collector
which is connected to a control valve. The control valve is connected
on the low-pressure side to the duct through which the air passes
into the heater. The required air pressure in the heater and in front
of the nozzle is maintained by the control valve.

A measuring diaphram was set up in front of the heater in order
to determine the flow rate of air.

3. Measured Quantities and Measuring Devices

The following quantities were measured during the experiment:
air pressure in front of the electrical heater and in front of the
working nozzle; air temperature at the heater outlet; static and
total pressure, temperature in the profiles of each section located
at a distance of 30 mm from the plane of the joint of the sections;
static pressure in two intermediate profiles of the first section in

the direction of air motion in which the pressure gradient is greatest; temperatures of the inner walls of the diffuser in the same profiles in which velocity, temperature, and static pressure of air flow are measured; temperature difference and water flow rate in all sections of the diffuser; pressure difference in the measuring diaphragm.

The air pressure in front of the heater and working nozzle was measured with a Burdon manometer having a measurement limit of 50 atm, division value of 0.25 atm and accuracy grade of 1.5. The pressure difference in the measuring diaphragm was measured with a DT-150 differential manometer. Total pressure in the boundary layer in the unperturbed flow in the sections in front of the cooled sections was measured with total-pressure pneumometric microtubes. One end of the Pitot tube faces toward the incident flow and the other is connected. to a differential manometer which is made in the form of a U-shaped tube filled with ethanol or water.

Static pressure was measured with a static-pressure sampling tube introduced to the inside of the passage through the wall. This tube is located in the same plane of the channel cross section in which the open end of the Pitot tube is located. The end of the static-pressure sampling tube is connected to a differential manometer. The second tube of this manometer is open to the atmosphere.

In order to determine the dynamic pressure, the Pitot tube and the static-pressure tube are connected to a differential manometer which records the difference of levels of the working fluids on its scale.

The Pitot tubes and thermocouples are set up by means of traverse gears which made it possible to measure the dynamic pressures and temperatures in the control profiles of the sections of the test

-5-

zone at 0.05 mm intervals. It is possible to measure the quantities mentioned at the corresponding points of all the five sections at the same time.

The flow temperature was measured by chromel-alumel thermocouples installed at a given distance from the wall by the traverse gear. Air temperature was recorded automatically on the tape of an electronic tape balancing potentiometer. The potentiometer was connected to 10 thermocouples, 5 of which measured the air-flow temperature and 5 the heat of the cooling water in the sectional housings.

The temperatures of the inner walls of the sections were measured with chromel-alumel thermocouples placed in machined grooves and carefully embedded flush to the air flow. Thermocouple readings were recorded with a potentiometer.

The temperature at the heater outlet was monitored by a chromel-alumel thermocouple connected to an electronic potentiometer type EPD.

ETA-5A electromanometers were also used to measure velocity, direction, and temperature of air flow.

4. Method of Treating Experimental Data.

In order to determine the variation of local friction values on the wall τ_w and unit heat flow at the wall q_w over the length of the diffuser, we used the integral relationships between momentum and energy which for axisymmetrical gas flow is written in the following form.

For momentum transfer

$$\frac{d\theta}{dx} + \left(\frac{\hslash + 2}{u_1} \cdot \frac{du_1}{dx} + \frac{1}{r} \cdot \frac{dr}{dx} + \frac{1}{\rho_1} \cdot \frac{d\rho_1}{dx} \right) \theta = \frac{\tau_w}{\rho_1 u_1^2}. \tag{1}$$

For energy transfer

$$\frac{d\varphi}{dx}+\left[\frac{1}{u_1}\cdot\frac{du_1}{dx}+\frac{1}{r}\cdot\frac{dr}{dx}+\frac{1}{T_{01}-T_w}\cdot\frac{d(T_{01}-T_w)}{dx}+\frac{1}{\rho_1}\cdot\frac{d\rho_1}{dx}\right]\varphi =$$

$$=\frac{q_w}{c_p\,\rho_1\,u_1\,(T_{01}-T_w)}\;;$$

(2)

where $\theta=\int\limits_0^{\delta}\dfrac{\rho u}{\rho_1 u_1}\left(1-\dfrac{u}{u_1}\right)\left(1-\dfrac{y\cos\beta}{r}\right)dy$ thickness of momentum loss;

$H=\dfrac{\delta^*}{\theta}\,;$ $\delta^*=\int\limits_0^{\delta}\left(1-\dfrac{\rho u}{\rho_1 u_1}\right)\left(1-\dfrac{y\cos\beta}{r}\right)dy$ displacement thickness;

u = velocity in the direction of the x-axis;

u_1= velocity at outer edge of the boundary layer;

x = distance, parallel to the wall;

r = radius (distance from the surface of axisymmetrical channel
     to its axis);

ρ_1= static density at the outer edge of boundary layer;

ρ = static density at a given point of boundary layer;

τ_w= tangential stress at wall;

q_w= specific heat flow at wall;

c_{p_*}=mass thermal capacity at constant pressure;

T_0 =adiabatic stagnation temperature in unperturbed flow ;

T_w= wall temperature;

$\varphi=\int\limits_0^{\Delta}\dfrac{\rho u}{\rho_1 u_1}\left(\dfrac{T_0^{\cdot}-T_0}{T_{01}-T_w}\right)\left(1-\dfrac{y\cos\beta}{r}\right)dy$ thickness of energy loss or thick-
     ness of enthalpy loss;

T_0= stagnation temperature at a given point in the boundary layer;

T_{01}=equilibrium temperature;

β = angle between the normal to the wall and the axis of the
     diffuser in the plane of the control profile;

δ = thickness of the dynamic boundary layer;

Δ = thickness of the thermal boundary layer.

All of the quantities which enter into Eqs. (1) and (2) with the

exception of τ_w and q_w were determined from experimental data for

constant values $\frac{dr}{dx}$ = 0.0705 and 0.105.

Velocity profiles and actual flow temperature profiles were calculated according to the measured temperature and dynamic pressure profiles.

Velocity was calculated by the formula

$$u = a^* \lambda,$$ (3)

where, for air,

$$a^* = 18,3 \sqrt{T_0};$$ (4)

$$\lambda = \sqrt{\frac{k+1}{k-1}\left[1 - \left(\frac{p}{p_0}\right)^{\frac{k-1}{k}}\right]}.$$ (5)

True air temperature was determined by the equation

$$T = T_{eq} - r\frac{u^2}{2gc_p I},$$ (6)

where T_{eq} = equilibrium temperature of the thermocouple

r = temperature recovery factor;

I = mechanical equivalent of heat.

A. A. Gukhman, N. V. Ilyukhin et al. [4] studied the dependence of the recovery factor r on Reynolds and Mach numbers M for a longitudinally streamlined thermocouple d = 0.5 mm placed in a tube with a diameter of 25 mm in the presence of a boundary layer. It was established that over the interval $3.8 \cdot 10^3 <$ Re$^* < 14.4.10^3$ and $0.24 <$ < M <0.98 the quantity r is a constant and equal to 0.90.

In our tests, longitudinally streamlined thermocouples with a wire diameter of 0.5 mm and junction diameter of 1.5 mm were used.

The values of Re* = $\frac{wd}{v}$ (where d is the wire diameter) varied from 900 to 10,000. Therefore, we assumed r = 0.90.

From the measured temperature and velocity profiles we determined the values of conditional boundary layer thicknesses θ, δ^*, and

φ of other quantities which enter into the integral relationships of momentum and energy $(u_1, \rho_1, (T_{01} - T_w),$ $\frac{d\vartheta}{dx}, \frac{d\varphi}{dx}, \frac{du_1}{dx}, \frac{d\rho_1}{dx}, \frac{d(T_{01} - T_w)}{dx}.$

Then the tangential stresses at the wall and the specific heat flows were calculated by Eqs. (1) and (2).

The reliability of determining the local values of τ_w and q_w by the described method depends substantially on the accuracy of the graphic differentiation of the original parameters. Therefore, local values of τ_w (or c_{fw}) and q_w were calculated by two independent methods. The method of determining c_{fw} is based on the well-known fact that the interior of the turbulent core of the boundary layer contains a universal logarithmic velocity profile which, in the presence of isothermic flow, is described by the equation

$$\frac{u}{v_*} = 5.75 \log \frac{y v_*}{\nu} + 5.5, \qquad (7)$$

where $v_* = \sqrt{\dfrac{\tau_w}{\rho}}$ - the dynamic velocity at the wall; and
ν = kinematic viscosity.

As is known, law (7) was obtained by integration of Prandtl's equation for tangential stress

$$\tau = \rho l^2 \left(\frac{du}{dy}\right)^2 \qquad (8)$$

for ρ = const, l = $\varkappa y$, τ = τ_w and with determination of the constant of integration and constant $\varkappa$ from measurements of velocity distribution made by I. Nikuradse.

To obtain a universal law of velocity distribution for a turbulent core in the presence of gas flow with heat transfer, it is necessary when integrating Eq. (8) to take into account the variation of density with temperature and to introduce a corresponding correction for heat transfer when determining the constant of integration.

Integrating Eq. (8), taking into account variation of gas density ($1 = \varkappa y$, $\tau = \tau_w$) we obtain

$$\frac{1}{\varkappa} \ln y = \frac{1}{v_*} \int \frac{du}{\sqrt{\frac{\rho_1}{\rho}}}.$$ (9)

Our measurements indicated that in the near-wall region we can assume

$$\frac{T_0 - T_w}{T_{01} - T_w} = \frac{u}{u_1}.$$ (10)

Taking into account (10), Eq. (9) reduces to the form

$$\frac{1}{\varkappa} \ln y = \frac{1}{\sqrt{\frac{c_{fw}}{2}}} \left[\frac{2\sqrt{\overline{T_w} + (1 - \overline{T_w})\frac{u}{u_1}}}{1 - \overline{T_w}} + C \right].$$

Taking $\varkappa = 0.4$ and determining the constant of integration C by joining the turbulent distribution of velocity with the laminar distribution of velocity in the immediate proximity of the wall where the laminar and turbulent tangential stresses are of the same order of magnitude, we obtain

$$2 \left[\frac{\sqrt{\overline{T_w} + (1 - \overline{T_w})\frac{u}{u_1}} - \sqrt{\overline{T_w}}}{1 - \overline{T_w}} \right] =$$

$$= \left[5.75 \log \left(Re_y \sqrt{\frac{c_{fw}}{2}} \right) + 5.5 \right] \sqrt{\frac{c_{fw}}{2}},$$ (11)

where $\overline{T_w} = \frac{T_w}{T_{01}}$; $Re_y = \frac{u_1 y}{\nu}$.

Constructing velocity profile (11) in variables $\frac{u}{u_1} = f(\frac{y}{\delta})$ for a given $\overline{T}$, we obtain a network of curves for fixed values of c_{fw}. If the experimental velocity values in the test cross section at a corresponding value of $\overline{T}_w$ are plotted on such a graph, then, according to the coincidence of the velocity profile in its logarithmic portion with one of the curves of the network, we will arrive at a corresponding value of c_{fw} which will also be a local value of the friction factor at the wall in the cross section under consideration.

Having completed such a construction for the various form parameters of pressure gradient

$$\Gamma = \left(\frac{\theta}{u_1}\cdot\frac{du_1}{dx}\right)\text{Re}_{\theta}^{1/4} = \left(-\frac{\theta}{\rho_1 u_1^2}\cdot\frac{dp}{dx}\right)\text{Re}_{\theta}^{1/4} \qquad (12)$$

(where $\text{Re}_{\theta} = \frac{u_1\theta}{\nu_1}$; ν_1- is the kinematic viscosity of the potential flow in the cross section under consideration), we were convinced that the logarithmic law of velocity distribution is preserved over approximately one-third of the boundary-layer thickness regardless of the pressure gradient.

An analogous construction was made for the temperature determination. A universal law of temperature distribution is preserved over a significantly greater portion of the thickness of the boundary layer than is the universal law of velocity distribution.

The second method of determining specific heat flow was the method of thermal equilibrium.

In order to determine the distribution of local values of tangential stress and specific heat flow over the cross section of the boundary layer, the differential equations of momentum and energy were integrated, taking into account the equation of continuity up to the current value of the y-coordinate.

The momentum equation is

$$\rho u \frac{\partial u}{\partial x} + \rho v \frac{\partial u}{\partial y} = -\frac{dp}{dx} + \frac{1}{r}\cdot\frac{\partial(r\tau)}{\partial y}; \qquad (13)$$

the equation of continuity is

$$\frac{\partial(r\rho u)}{\partial x} + \frac{\partial(r\rho v)}{\partial y} = 0; \qquad (14)$$

and the energy equation is

$$\rho u \frac{\partial T_0}{\partial x} + \rho v \frac{\partial T_0}{\partial y} = \frac{1}{gc_p r}\cdot\frac{\partial(rq)}{\partial y}, \qquad (15)$$

where $\underline{x}$ and $\underline{y}$ are coordinates directed along and normal to the flow

respectively; $\underline{u}$ and $\underline{v}$ are the normal and tangential components of velocity. After integrating Eqs. (13), (14) and (15) integral equations of momentum and energy were obtained for a boundary layer of thickness from 0 to $\underline{y}$.

The momentum equation is

$$\frac{d\theta_y}{dx} + \left(\frac{2+H_y}{u_1} \cdot \frac{du_1}{dx} + \frac{1}{r} \cdot \frac{dr}{dx} + \frac{1}{\rho_1} \cdot \frac{d\rho_1}{dx}\right)\theta_y -$$

$$- \frac{u_1-u}{r\rho_1 u_1^2}\int_0^y \frac{\partial(r\rho u)}{\partial x} dy = \frac{\tau_w}{\rho_1 u_1^2} - \left(1 - \frac{y\cos\beta}{r}\right)\frac{\tau_y}{\rho_1 u_1^2}. \qquad (16)$$

The energy equation is

$$\frac{d\varphi_y}{dx} + \left[\frac{1}{u_1} \cdot \frac{du_1}{dx} + \frac{1}{r} \cdot \frac{dr}{dx} + \frac{1}{\rho_1} \cdot \frac{d\rho_1}{dx} + \frac{1}{T_{01}-T_w} \cdot \frac{d(T_{01}-T_w)}{dx}\right]\varphi_y -$$

$$- \frac{T_{01}-T_0}{r\rho_1 u_1(T_{01}-T_w)}\int_0^y \frac{\partial}{\partial x}(r\rho u)\, dy = \frac{1}{gc_p\rho_1 u_1(T_{01}-T_w)} \times \qquad (17)$$

$$\times \left(q_w - \frac{r_y}{r}q_y\right),$$

where $\theta = \int_0^y \frac{\rho u}{\rho_1 u_1}\left(1 - \frac{u}{u_1}\right)\left(1 - \frac{y\cos\beta}{r}\right) dy$ the thickness of momentum loss for a fixed value of $\underline{y}$; and $\delta_y^* = \int_0^y \left(1 - \frac{\rho u}{\rho_1 u_1}\right)\left(1 - \frac{y\cos\beta}{r}\right) dy$ the displacement thickness for a fixed value of $\underline{y}$.

Equation (16) is used to calculate the distribution of friction factor c_f over the cross section of the boundary layer with the substitution of experimental values of the magnitudes which enter into it. Heat flows for a fixed value of $\underline{y}$ in the boundary layer are calculated from Eq. (17).

According to the calculated distributions of the friction factors and heat flows in the cross section of the boundary layer, the corresponding values of the coefficients of turbulent momentum and heat transfer A_τ and A_q were determined from the equations

$$A_\tau = \frac{\tau}{\frac{du}{dy}}, \qquad (18)$$

$$A_q = \frac{q}{gc_p\frac{dT}{dy}}. \qquad (19)$$

5. Results of the Experimental Investigations

The measurements of temperature, total and static pressure, and heat flow in five insulated sections of the experimental diffuser were made under 22 regimes of motion of heated air and in 4 regimes with unheated air. Each regime is characterized by a definite air temperature and velocity at the entrance profile of the test section. A change of entrance air parameters by regimes made it possible to significantly alter the flow rate of air and the Reynolds number. The experiments encompassed Reynolds numbers $(1.688 + 8.48)\,10^5$ and air flows of 0.35 to 1.37 kg/sec.

The presence of well-insulated flow stabilization sections and also of two metal nets in front of test section assured equalization of the velocity and temperature fields over the flow cross section. The origin of growth of the boundary layer in all experimental regimes was related to the entrance cross section of the cooled diffuser.

6. Analysis of Experimental Data ·

Figures (3) and (4) show the temperature and velocity distribution over the cross section of the boundary layer for various values of the form parameter Γ. It is apparent from these graphs that the velocity profiles in the diffuser become less filled with an increase in pressure gradient. The same tendency, though to a significantly smaller degree, is observed in individual temperature determinations. From a comparison of the graphs of velocity and temperature distribution it follows that in gas flow with a positive pressure gradient, there is no similarity of velocities and temperatures. An especially significant disruption of similarity of these fields is observed in the pre-separation region.
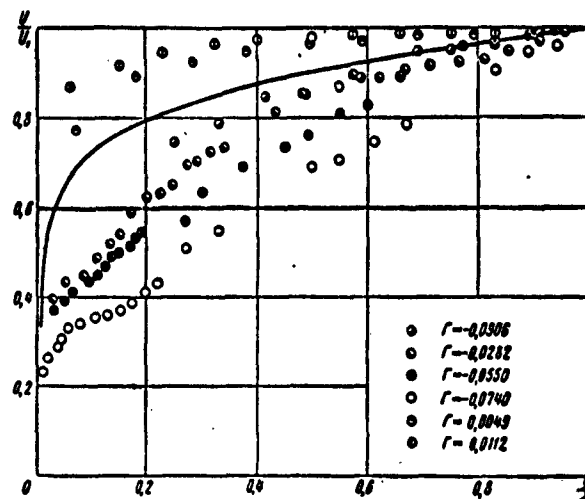
Fig. 3.   Distribution of velocity over
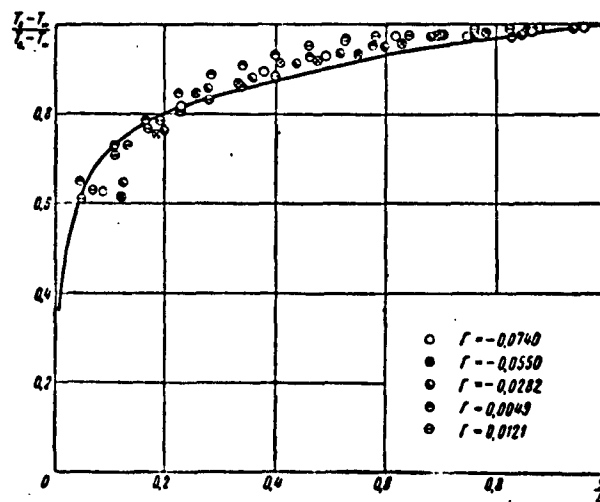the cross section of the boundary layer.

Fig. 4.   Distribution of temperature over
the cross section of the boundary layer.

Figure 5 shows the dependence of the form parameter $H = \dfrac{\delta^*}{\theta}$

(with calculation of θ in the variables of A. Dorodnitsyn) on Γ.

This graph shows that H uniquely depends on Γ, where upon the function

$H = f(\Gamma)$ is independent of the Reynolds number. Therefore, the form parameter Γ expressed by Eq.(12) is a useful form parameter for the study of the behavior of the turbulent boundary layer in the presence of a flow gradient with heat transfer.

The connection between the quantities H and Γ is expressed by equation
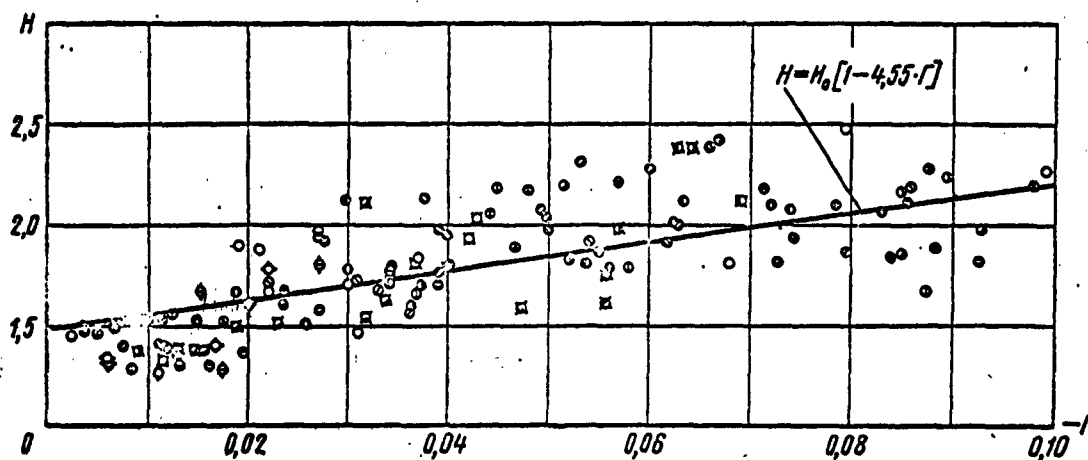
$$H = 1{,}47\,(1 - 4{,}55\,\Gamma).$$
(20)

Fig. 5. H vs. f(-Γ).

It is important to note that boundary-layer separation is not observed up to form parameter values greater than twice the separation values of $\Gamma = 0.06$ according to A. Buri. Accordingly, the values of H obtained in experiments reach 2.5, which approaches the separation values of H recommended by A. E. Doenhoff and N. Tetervin [8]. The actual protraction of the separation point in comparison with the motion of uncompressed fluids is explained by a number of causes: the stabilizing influence of the cooled walls of the diffuser, the axisymmetrical flow under our conditions and also by the fact that in the experiments of I. Nikuradse [5], the results of which were the basis of Buri's determination of the separation value of Γ, the boundary layer fills the entire cross section of the channel, whereas our experiments were conducted with a potential flow over a significant portion of the passage.

The scattering of experimental points on the graph of H = $f(\Gamma)$ may be explained by the influence of different cooling conditions. Apparently, the determination of H with respect to the thickness of momentum loss in the variables of A. Dorodnitsyn does not permit total elimination of the heat transfer effect.

In order to obtain a closed system of equations which establish a connection between the characteristics of the dynamic boundary layer, we need an additional form parameter which defines a law of friction. On the basis of the experimental data of I. Nikuradse [5], A. Buri showed that with a flow gradient of an uncompressed fluid without heat transfer, the law of friction may be expressed by the equation

$$\zeta = \frac{\tau_w}{\rho_1 u_1^2} Re_\delta^{1/4} ,$$

(21)

since under these conditions ζ is a single-valued function of the form parameter Γ, this function, like the function $H(\Gamma)$, is independent of

the Reynolds number.

When we generalized our experimental data on resistance it became clear that the quantity ζ expressed by Eq. (21) may be used to establish a law of friction also in the presence of a gas flow gradient with heat transfer if the temperature factor $\overline{T}_w$ is introduced into the functional dependence $\zeta = f(\Gamma)$.

In the first approximation the influence of heat transfer on ζ was calculated according to the limit formula obtained in the literature [16(sic)].

Figure 6 shows the dependence $\zeta\left(\dfrac{\sqrt{\overline{T}_w}+1}{2}\right)$ on Γ with determination of ζ and Γ by Eqs. (21) and (12). The significant scattering of experimental points on this graph is apparently explained by the fact that the indicated limit formula was obtained for a nongradient gas flow.

The experimental points in Fig. 6 are satisfactorily distributed along the curve of the equation

$$\zeta\left(\frac{\sqrt{\overline{T}_w}+1}{2}\right)^2 = 0,0128(1-\Gamma)^{-20}. \tag{22}$$

Taking Eq. (21) into account, we obtain a law of resistance

$$\frac{\tau_w}{\rho_1 u_1^2} = \frac{c_{fw}}{2} = \frac{0,0128}{Re_\delta^{1/4}}\left(\frac{2}{\sqrt{\overline{T}_w}+1}\right)^2\frac{1}{(1-\Gamma)^{20}}. \tag{23}$$

Experimental data encompassing a variation of the temperature factor from 0.5 to 1, and values of form parameter Γ from 0 to 0.12 was used in plotting the graph in Fig. 6.

Figure 7 shows the dependence of form parameter H on the form parameter η introduced by Gruschwitz [2]:

$$\eta = 1 - \frac{u^2(\theta)}{u_1^2}, \tag{24}$$

which is associated with the form parameter $H = \dfrac{\delta^*}{\theta}$ by the equation

$$\eta = 1 - \left[\frac{H-1}{H(H+1)}\right]^{H-1} = 1 - \left(\frac{\theta}{\delta^*}\right)^{2/n}, \qquad (25)$$

obtained according to the exponential law of velocity distribution

$$\frac{u}{u_1} = \left(\frac{y}{\delta}\right)^{1/n},$$

where $u(\theta)$ is the velocity within the boundary layer at a distance $y = \theta$ from the wall;
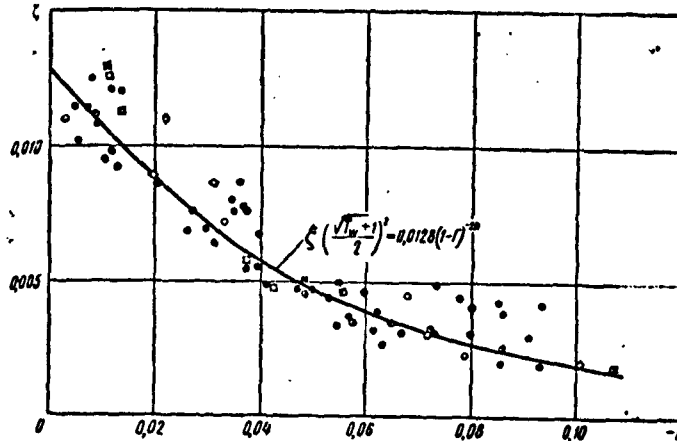
$$n = \frac{2}{H+1}.$$

Fig. 6. ζ vs. $f(-\Gamma)$.

In addition to our own, experimental points from Gruschwitz [2], Nikuradse [5], and Kehl [6] are plotted in Fig. 7. It is apparent from the graph that the experimental points of Gruschwitz, Nikuradse and Kehl lie nicely on the Gruschwitz curve (Eq. 25) in the region of small values of the form parameter H. Our experimental points cover a range of larger values of the form parameters H and η, in which we observe a significant deviation of experimental points from the Gruschwitz dependence.

Figure 8 shows the variation along the longitudinal coordinate of local values of the resistance coefficient c_{fw} at the wall for one of the regimes (regime 13) of our experiments. The curves of variation

of the resistance coefficients for the corresponding conditions based
on the methods of Buri and Ye. Kalikhman are also plotted. As can
be seen from the graph, the greatest deviation from experimental
points is produced by the Kalikhman method which is based on the
analogy between processes of heat and momentum transfer in a boundary
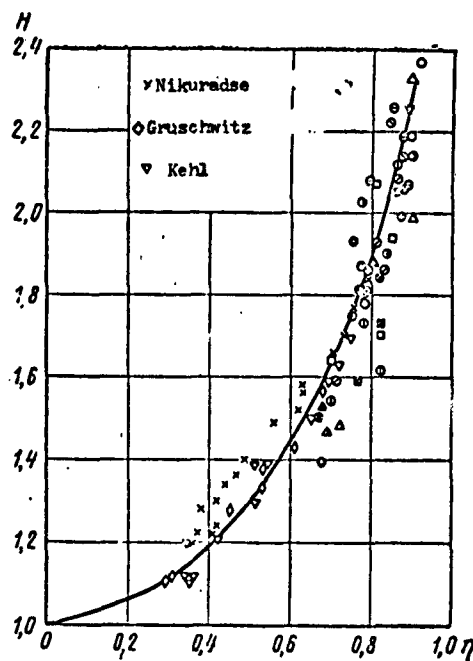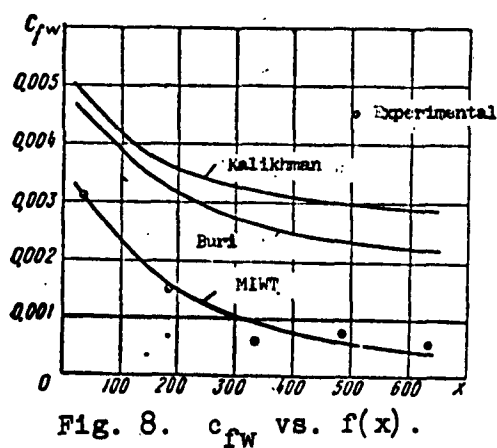layer.

Fig. 7. H vs. f(η)

Fig. 8. c_{fw} vs. f(x).

7. Dynamic Turbulent Boundary Layer Calculation.

Let us represent Eq. (1) in the following form:

$$\frac{dRe_{\theta}}{d\bar{x}} + (H+1)\frac{Re_{\theta}}{u_1}\cdot\frac{du_1}{d\bar{x}} + \frac{1}{r}\cdot\frac{dr}{d\bar{x}}Re_{\theta} = \frac{\tau_w Re_L}{\rho_1 u_1^2}, \qquad (26)$$

where $\bar{x} = \frac{x}{L}$; $Re_L = \frac{\rho_1 u_1 L}{\mu_{\infty}}$; L = characteristic length of measure; and μ_{∞} = = coefficient of dynamic viscosity of the potential flow at stagnation temperature.

Taking into account Eq. (21), Eq. (26) is reduced to the form

$$\frac{d}{d\bar{x}}\left(Re_{\theta}^{5/4}\right) + \frac{5}{4}\cdot\frac{1}{r}\cdot\frac{dr}{d\bar{x}}Re_{\theta}^{5/4} = \frac{5}{4}Re_L[\zeta-(H+1)\Gamma]. \qquad (27)$$

We will designate $F(\Gamma) = \frac{5}{4}[\zeta-(H+1\Gamma]$.

Figure 9 shows the dependence of the function $F(\Gamma)$ on form parameter Γ. The values of $F(\Gamma)$ calculated from the values of ζ, H, and Γ obtained in our experiments are nicely arranged along the line

$$F(\Gamma) = 0.0155 - 3.55\,\Gamma. \qquad (29)$$

Thus, although the quantities ζ and H substantially depend on heat transfer the latter, as was to be expected, has practically no effect on the function $F(\Gamma)$.

Taking into account Eq. (29) and substituting Γ by means of its expression (12), Eq. (27) is transformed into a differential equation of the first order with respect to $Re_{\theta}^{5/4}$. Integrating this equation and solving for Re_{θ} we obtain

$$Re_{\theta} = \left[\frac{0.0155}{r^{1.25}u_1^{3.55}}\left(\int_{\bar{x}_H}^{\bar{x}}Re_L r^{1.25}u_1^{3.55}d\bar{x}+C\right)\right]^{0.8}, \qquad (30)$$

where C, the constant of integration is

$$C = \left[\frac{Re_{\theta}^{1.25}r^{1.25}u_1^{3.55}}{0.0155}\right]_{\bar{x}=\bar{x}_H};$$

and $\bar{x}_H$ is the value of the dimensionless coordinate x of the starting

-20-

point of the turbulent boundary layer under consideration.
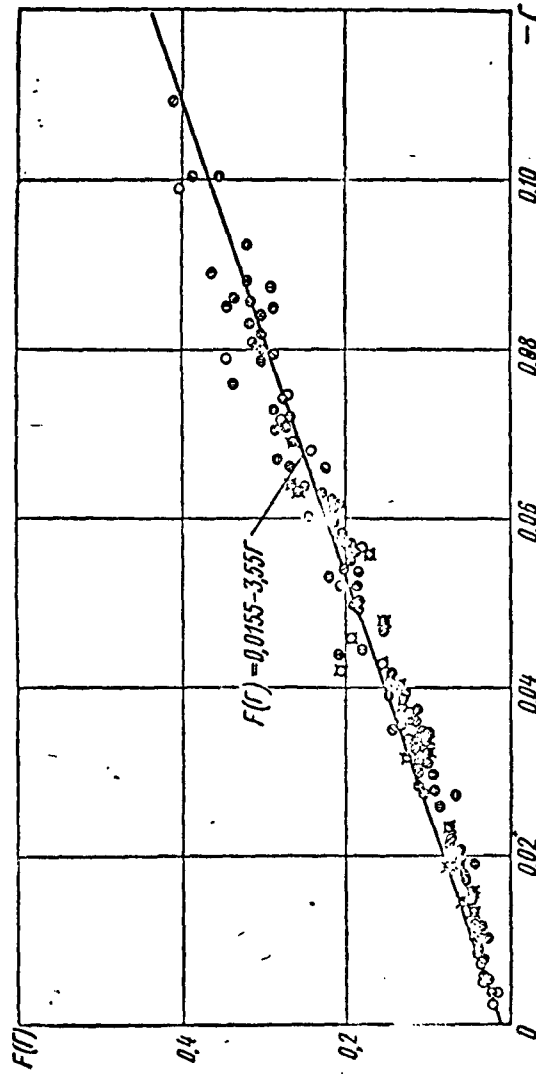

Fig. 9. $F(\Gamma)$ vs. $f(\Gamma)$

On the basis of the data obtained, their treatment, and generalization, which made it possible to integrate the equation of motion, we can recommend the following sequence of calculation of a dynamic boundary layer with turbulent gas flow in an axisymmetrical channel with a longitudinal pressure gradient and with heat transfer:

1. With   given laws of velocity and temperature variation of the potential flow and a given channel radius along the longitudinal coordinate $\underline{x}$, the Re_θ number, established over the thickness of momentum loss is determined according to Eq. (30) as a function of $\underline{x}$ and, consequently, a dependence of momentum loss thickness θ as a function of $\underline{x}$ is determined.

2. The magnitude of the form parameter Γ as a function of $\underline{x}$ is determined according to Eq. (12).

3. The local value of the resistance coefficient at the wall as a function of $\underline{x}$ is determined according to Eq. (23) for a given law of wall temperature with respect to the coordinate $\underline{x}$ and for a known temperature recovery factor for the potential flow.

4. The magnitude of the form parameter H as a function of $\underline{x}$ is determined according to Eq. (20).

This method of calculation must be used in a region of relatively small temperature factors ($\overline{T}_w$ = 0.5 to 1). The question of the influence of more intense cooling or heating on the characteristics of the turbulent boundary layer will be studied in the future.

8.   Thermal Boundary Layer Calculation

The thermal boundary layer is calculated on the basis of an integral equation of energy and on experimental data concerning the distribution of temperature in the boundary layer and the variation

of the temperature of the channel walls.

Equation (2) is easily reduced to the form

$$\frac{d}{dx}(r\text{Re}_\varphi^{5/4}) + \frac{1}{4}\cdot\frac{1}{r}\cdot\frac{dr}{dx}(r\text{Re}_\varphi^{5/4}) + \frac{5}{4}\cdot\frac{1}{T_{01}-T_w}\cdot\frac{d(T_{01}-T_w)}{dx}\times$$

$$\times (r\text{Re}_\varphi^{5/4}) = \frac{5}{4}r\text{Re}_L\,\text{St}\,\text{Re}_\varphi^{1/4}, \qquad (31)$$

where

$$\text{Re}_\varphi = \frac{u_1\varphi}{\gamma_1};\ \ \text{St} = \frac{q_w}{c_p\,\rho_1\,u_1\,(T_{01}-T_w)}.$$

Treatment of our experimental data on the temperature distribution indicated that the values of the product $\text{St}\,\text{Re}_\varphi^{1/4}$, laid out as ordinates for the values of the form parameter Γ_T of the thermal boundary layer with a pressure gradient equal to

$$\Gamma_T = \frac{\varphi}{u_1}\cdot\frac{du_1}{dx}\text{Re}_\varphi^{1/4} = \left(-\frac{\varphi}{\rho_1 u_1^2}\cdot\frac{dp}{dx}\right)\text{Re}_\varphi^{1/4}, \qquad (32)$$

are well distributed on a line parallel to the abscissa (Fig. 10), thus indicating an independence of the product $\text{St}\,\text{Re}_\varphi^{1/4}$ on the pressure gradient. The average value of $\text{St}\,\text{Re}_\varphi^{1/4}$ in the graph of Fig. 10 may be taken as equal to 0.01.
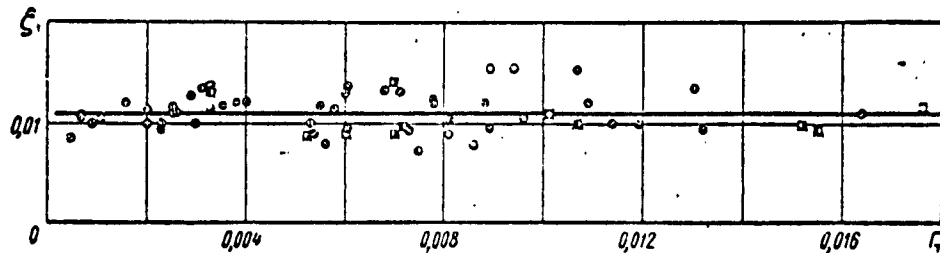
Fig. 10. ζ_T vs. $f(\Gamma_T)$.

Substituting the value 0.01 for $\text{St}\,\text{Re}_\varphi^{1/4}$ in Eq. (31) we obtain

$$\frac{d}{dx}(r\text{Re}_\varphi^{5/4}) + \left[\frac{1}{4}\cdot\frac{1}{r}\cdot\frac{dr}{dx} + \frac{5}{4}\cdot\frac{1}{T_{01}-T_w}\cdot\frac{d(T_{01}-T_w)}{dx}\right]\times$$

$$\times (r\text{Re}_\varphi^{5/4}) = 0.0125r\,\text{Re}_L. \qquad (33)$$

Integrating Eq. (33) with respect to $r\text{Re}_\varphi^{5/4}$ and then expressing the resulting integral with respect to Re_φ we find

$$Re_i = \left\{ \frac{0,0125}{r^{5/4}(T_{01}-T_w)^{5/4}} \cdot \left[\int_{x_H}^{x} r^{5/4}(T_{01}-T_w)^{5/4} Re_L \, d\bar{x} + C \right] \right\}^{0,8}. \qquad (34)$$

where C, the constant of integration is

$$C = \left[\frac{r \, Re_i (T_{01}-T_w)}{0,03} \right]^{1,25}_{x=x_H}.$$

The Stanton number as a functional $\underline{x}$ is determined according to the equation

$$St = \frac{0,01}{Re_i^{1/4}}. \qquad (35)$$

The thermal boundary layer for turbulent gas flow in an axisymmetrical channel with a longitudinal pressure gradient is calculated in the following sequence:

1. With given laws of velocity and temperature variation in a potential flow as well as a given wall temperature and channel radius along the longitudinal coordinate $\underline{x}$, $Re_\varphi(x)$ and then the dependence of the energy loss thickness $\varphi(x)$ are determined by Eq. (34). In the case when no analytical law is given for velocity and temperature variation in the potential stream as well as for wall temperature variation, Eq. (34) may be integrated numerically.

2. Values of the form parameter Γ_T as a function of $\underline{x}$ are found from Eq. (32) .

3. Values for Stanton number are calculated by Eq. (35) .

4. Thermal flow at the wall of the channel is calculated by equation

$$q_w = c_p \rho_1 u_1 (T_{01} - T_w) St. \qquad (36)$$

5. The relation between the form parameters Γ and Γ_T is established on the basis of Eqs. (12) and (32) .

-24-

9. Reynolds' Analogy on Heat and Momentum Transfer

The experimental data obtained makes it possible to analyze the question of the accuracy of the analogy in the processes of heat and momentum transfer in the presence of a pressure gradient.

The original premises for Reynolds' analogy, as is well-known, are the equality of the coefficients of turbulent heat and momentum transfer as well as the identity of the laws of variation of τ and $\underline{q}$ over the cross section of the boundary layer. The result of these premises is the similarity of the velocity and temperature profiles in the boundary layer.

A significant breach in the similarity of the velocity and temperature profiles in the boundary layer with a positive pressure gradient is pointed out above. In order to clarify the causes of this breach it is necessary to varify the accuracy of the original premises of Reynolds' analogy under conditions of a gas flow gradient. Figure 11 shows the distribution of τ and $\underline{q}$ over the cross section of the boundary layer obtained by the calculation method described above. As can be seen from the graph, the laws of variation of τ and $\underline{q}$ over the cross section of the boundary layer in the presence of a gas flow gradient significantly differ, the difference being greater the nearer flow conditions are to separation. A characteristic maximum with a subsequent drop to zero at the outer edge of the boundary layer is observed in the distribution of τ in proportion to the distance from the wall. The magnitude of specific thermal flow drops continuously from maximum at the wall to zero at the outer edge of the boundary layer. Thus, one of the premises of Reynolds' analogy is not verified by the experiments with a gas flow gradient.
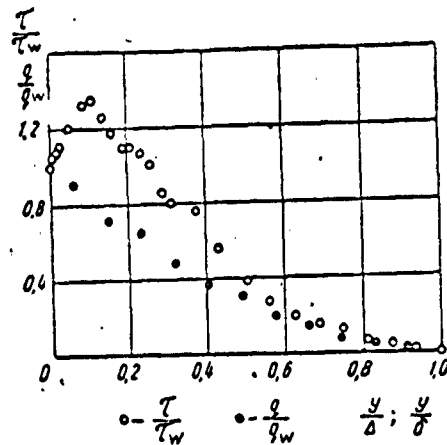
Fig. 11. Distribution of heat flow
and frictional stress over the cross
section of the boundary layer (regime
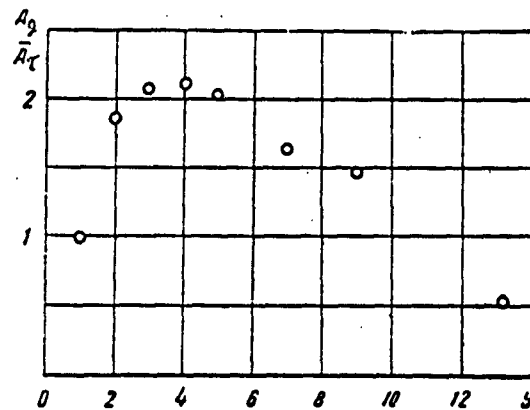12, cross section 2).

Fig. 12. Distribution $\dfrac{A_q}{A_\tau}$ of the cross

section boundary layer (regime 12, cross
section 2).

Figure 12 shows the variation of the relationship of the coeffi-
cients of turbulent momentum and heat transfer (turbulent Prandtl
number) over the cross section of the boundary layer. From Fig. 12

it follows that near the wall, the coefficients A_q and A_τ are the same. The coefficient of turbulent heat transfer exceeds the coefficient of momentum transfer in proportion to the distance from the wall, and at some distance from the wall A_q is approximately twice A_τ. Subsequently the ratio A_q/A_τ drops in proportion to distance from the wall. Consequently the second premise of Reynolds' analogy (on the equality of the coefficients A_q and A_τ) is also not confirmed by experimental data.

The regularity of the variation of A_q/A_τ over the cross section of the boundary layer which we obtained, is in qualitative agreement with experimental data of Ludwing [9], Elias [10], and Feydzh and Fokner [11]. In particular, the latter obtained $A_q/A_\tau = 2$ on the basis of the measurement of temperature and velocity distribution in a free flow. It may be assumed that at some distance from the wall the mechanism of heat and momentum transfer obeys the regularities of free turbulence. From the physical point of view the influence of free turbulence must predominate in proportion to the nearness of the points of separation, since in this case the influence of the wall on the characteristic of turbulence in the boundary layer decreases.

The analysis which was carried out indicates that the Reynolds analogy is not verified for gas motion with a longitudinal pressure gradient. Consequently all of the analytical methods of calculating the turbulent boundary layer which are based on the. use of Reynolds' analogy, Kalikhman's in particular, cannot be extended to the case of gas motion with a significant positive pressure gradient.

Conclusions

1. As a result of the experimental studies carried out, new

experimental data were obtained on the characteristics of a turbulent
boundary layer with gas motion in an axisymmetrical diffuser with
cooled walls.

2. Analysis of the experimental data obtained indicated that
existing methods of turbulent boundary layer calculation (of Buri,
Gruschwitz and Kalikhman) are not verified by experiments with gas
motion in an axisymmetrical diffuser with cooled walls.

3. Experimental values of the form parameter Γ corresponding to
the separation point of a turbulent boundary layer significantly
exceed the corresponding values according to the data of I.
Nikuradse.

4. Experimental values of the form parameter ζ lie between
the corresponding values obtained by the methods of Buri and Gruschwitz.

4. Experimental data were obtained on the dependence of the form
parameter H on the Gruschwitz form parameter η in a region which was
not previously covered by experimental data.

6. Analysis of experimental data indicated that the Buri method
may be extended to the case of gas motion in an axisymmetrical diffuser
with cooled walls by the introduction of suitable refinements for
the graphs of $H = f(\Gamma)$; $\zeta = f(\Gamma)$ and $F(\Gamma) = f(\Gamma)$.

7. The proposed method of calculation is found to be in good
agreement with experimental data both with regard to the calculation
of the integral characteristics of the turbulent boundary layer and
to local values of the coefficient of friction.

8. Of the existing methods of turbulent boundary layer calcu-
lation, the method based on the premises of Reynolds analogy (the
method of L. Ye. Kalikhman) gives the greatest divergence from experi-
ments.

9. Experiments indicated that with a gradient of gas motion there is observed a significant breach of similarity between the velocity and temperature profiles.

10. The ratio q/τ cannot be taken as constant over the cross section of the boundary layer with a gradient of gas motion.

11. The ratio of the coefficients of turbulent heat and momentum transfer A_q/A_τ varies significantly over the cross section of the boundary layer from $A_q/A_\tau = 1$ at the wall to $A_q/A_\tau = 2$ in the main section of the turbulent boundary layer.

REFERENCES

1. A. Buri., Eine Berechnugsgrundlage fur die turbulente Grenzschicht der beschleuigter und verzogerter Stromung, Dissertation, Zurich, 1931.

2. E. Gruschwitz., Die turbulente Reibungsschicht in ebener stromung mit Druckabfall und Druckanstieg, Ind. - Arch., 2 (1931), 321.

3. F. H. Clauser., Turbulent boundary layer in adverse pressure gradients. I. A. S., 21, No. 2, 91-108, 1954.

4. A. A. Gukhman, N. V. Ilyukhin, L. N. Naurits and A. F. Gendel'sman, Eksperimental'noye issledovaniye prodol'no-obtekayemoy termopary pri techeniy gaza s bol'shoy skorost'yu, TsKTI im. Polzunova. Teploperedacha i aerodinamika, kn. 21, Mashgiz, 1951.

5. I. Nikuradse., Untersuchungen uder die stromungen des Wassers in konvergenten und diwergenter Kanalen, Forschungsarbeiten des V. D. I., 289, 1929.

6. A. Kehl., Uber konvergente und divergente turbulente Reibungsschichten, Lng - Arch 12, 1943, 293.

7. I. Pretsch., Zur teoretischen Berechnung des Profilwiderstandes, Ib. d. dt. Iuftfahrtforschung, 1938, I. 61.

8. A. E. Doenhoff and N. Tetervin., Determination of general relations for the behavior of turbulent boundary layers, N.A.C.A., Rep. 772, 1943.

9. H. Ludwing., Zs. Flufuiss., 4 Nr 1-2, 73-81, 1956.

10. F. Elias., Zs. angew. Math. Mech. 9, 434-453, 1929, 10, 1-14, 1930.

11. <u>G. I. Taylor.</u>, The transport of vorticity and heat through fluids in <u>turbulent motions</u> dobavleniyem A. Feygzha u V. M. Foknera, 135, 1932. 685.

12. <u>D. A. Spence</u>., The development of turbulent boundary layers, Journal of the Aeronautical Sciences, vol. 23, Nr 1, 1956.

13. <u>E. Van Draist</u>., Turbolentniy nogranichnyy sloy v ozhimay-emykh zhidkostyakh. Sb. Mekhanika", Nr 1/11, 1952.

14. <u>Szablewski.</u>, Ingenier - Archiv Bd. XXII Heft. 4, 1954; Bd, XIII, Heft 4, 1955.

15. <u>S. S. Kutateladze and A. I. Leont'yev.</u>, Turbolentnyy pogranichnyy sloi szhimayemogo gaza na ploskoy plastine. Prikladnaya mekhanika i tekhnicheskaya fisika Nr 4, 19560.

DISTRIBUTION LIST

DEPARTMENT OF DEFENSE	Nr. Copies	MAJOR AIR COMMANDS	Nr. Copies
		AFSC	
		DCFDD	1
		DDC	25
HEADQUARTERS USAF		TDBTL	5
		TDBDP	5
AFCIN-3D2	1	AEDC (AEY)	1
ARL (ARB)	1	SSD (SSF)	2
		AFFTC (FTY)	1
		AFSWC (SWF)	1
OTHER AGENCIES		ASD (ASYIM)	1
A	1		
	6		
	9		
AID	2		
OTS	2		
AEC	2		
PWS	1		
NASA	1		
ARMY (FSTC)	3		
NAVY	3		
NAFEC	1		
RAND	1		
PGE	12		